ECCM 2010
IV European Conference on Computational Mechanics
Palais des Congrès, Paris, France, May 16-21, 2010

Model validation of the numerical simulation of the Double Punch Test

A. Pros[1,2], P. Díez[1,2], C. Molins[1]

[1]*Escola Tècnica Superior d'Enginyers de Camins, Canals i Ports de Barcelona (ETSECCPB)*
Universitat Politècnica de Catalunya (UPC), Barcelona, Spain
[2]*Laboratori de Càlcul Numèric (LaCàN)*
{alba.pros,pedro.diez,climent.molins}@upc.edu

Key words: Double punch test, numerical simulation, nonlocal damage model, joint elements, model validation.

Summary. The Double Punch test, an indirect traction test, is simulated numerically considering two different models (the nonlocal Mazars damage model and an heuristic crack model with joint elements). The test was designed to measure indirectly the tensile strength of concrete, hence, through these two numerical models, we are able to assess the tensile strength numerically. Experimental results present scattering when assessing the tensile strength, therefore, other tests are needed to set all the material and geometrical parameters of the numerical models. Both models are validated for the Double Punch test.

1 INTRODUCTION

The Double Punch Test (DPT) is used to indirectly measure the tensile strength of plain concrete. Experimental results are available and the numerical simulation has been carried out based on these results.

The information extracted from the experimental tests is translated into the parameters characterising the mechanical properties of the analysed concrete. In this case, the parameter to be assessed is precisely the tensile strength. Essentially, the data provided by the experimental setup is a force-displacement curve in which the peak points corresponding to the collapse are easily identified. The force corresponding to the peak point is readily translated into a tensile strength using a theoretical model simulating the mechanical behavior of the test. Up to now, the theoretical model used in this framework is an analytical solution of the linear elastic problem [1, 2]. These models are a crude approximation of the actual behavior of the specimen close to the collapse regime but they still provide a good approximation of the tensile strength by selecting a characteristic tensile stress in the linear elastic solution for the peak force.

In this work, the use of more accurate theoretical models is advocated. The idea is to replace the naif linear elastic model by a more realistic one that has the maximum tensile strength already as one of material parameters and to identify the value of this material parameter that better fits the experimental results.

Two different approaches are considered in order to model the mechanical behavior of the concrete in the DPT. Firstly (option A), a continuous model that has been successfully used modeling the popular Brazilian test [3], the nonlocal Mazars damage model. Secondly (option B), a model is selected that introduces discontinuous fracture at the fracture surfaces corresponding to an a priori defined fracture pattern, based on the experimentally observed fracture mechanisms. Along the fracture surfaces, joint elements with cohesive dilatant behavior are used to model the interfaces. In the rest of the specimen,

the mechanical behavior is assumed to be linear elastic because the relevant deformation is concentrated in the fracture surfaces. Obviously, both options A and B rely on the use of numerical models. Here, 3D finite element approximations are used complemented (for option B) with 2D joint elements.

Different variations have to be explored for option B (heuristic cracking model): the influence of the different a priori defined fracture patterns (basically the number of fracture planes) is studied.

Both options A and B provide approximations of the pre-peak and the post-peak behavior. Therefore, the information that may be extracted from the numerical tests to identify the parameters is here richer than in the previous attempts.

The goal of this study is to analyze the features of the different models and their capabilities to properly approximate the experimental tests by fitting the experimental data available. An objective comparison is performed by setting a measure of the error between the experimental data and the model. This results in fact in setting a fitting criterion. Correspondingly, the parameter identification and the model validation are carried out both based on the same criterion.

As a consequence of this analysis, the tensile strength f_t is identified with different methodologies. The detailed analysis of the obtained results together with the model validation yields an indication on which of the values of f_t is preferable.

All the experimental results are from an experimental campaign which consists of reproducing the double punch test. However, considering the same concrete (same material parameters) other tests are reproduced in the same campaign. Hence, experimental data is available not only from the double punch test, but also from two different tests.

Thus, sophisticated models are used to identify the tensile strength from the DPT, instead of the linear elastic model. The advantage of using this approach is more relevant when DPT is used to identify the tensile behavior of steel fiber reinforced concrete, not with plain concrete. For fiber reinforced concrete, taking into account also the pre- and post-peak behavior (and not only the peak) is extremely relevant. The present work has to be seen as a first step towards including steel fibers into these models in order to simulate the DPT for steel fiber reinforced concrete (a test introduced in [18], defined as the Barcelona Test).

2 DESCRIPTION OF THE DOUBLE PUNCH TEST

As introduced in [1, 2, 4], the Double Punch Test was proposed in [5, 6, 7] in order to measure indirectly the tensile strength of plain concrete. It was presented as an alternative to the Brazilian test, which was so far the most popular indirect traction test.

The test layout is illustrated in figure 1 and consists in compressing a cylindrical concrete specimen with two steel circular punches centered at the plane sides (top and bottom). The geometry of the specimen is given by the height ($l = 15$cm) and the diameter ($d = 15$cm). The ratio between the diameters of the punches and the specimen is one fourth ($d' = \frac{1}{4}d = 3.75$cm). Moreover, the applied load value corresponds to P.

A typical failure mechanism presents three radial fracture planes. However, in the experimental results, the observed number of fracture planes ranges from two to four. The geometry of the collapse pattern is completed with two fracture cones beneath each punch. In figure 2 two different fracture patterns are illustrated.

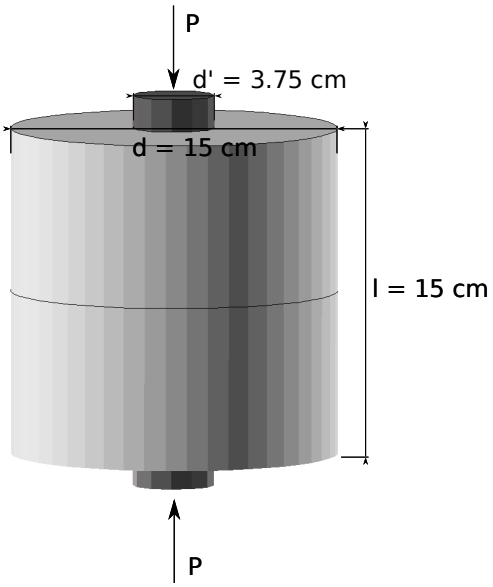

Figure 1: Double Punch Test layout

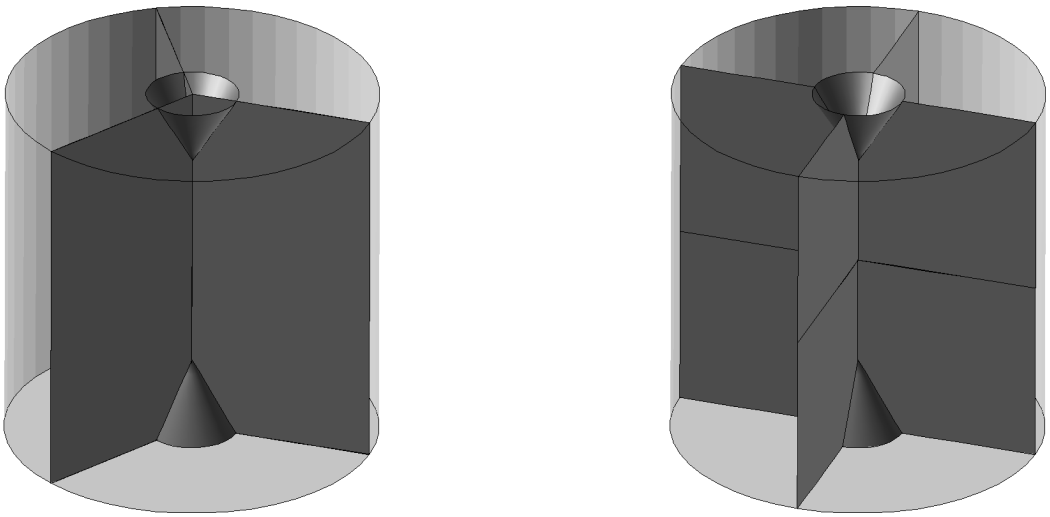

Figure 2: Two possible collapse mechanisms with three and four radial fracture planes

Comparing DPT to the Brazilian test, DPT is a a reduced size test easier to perform. Moreover, the calculated tensile strength in the DPT gives an average value of the tensile strength on several cracked diametral planes, meanwhile, the Brazilian test confines failure to a predetermined plane.

The test is controlled by the vertical displacement between the plates of the press at a 0.5 mm/min rate imposed at the punches.

During this work, the size of the specimen is fixed. For a fixed geometric ratio, the importance of the size effect on tensile strength in the DPT is studied in [6]. However, the tensile strength interpreted from the DPT is relatively insensitive to the shape of the specimen.

Tensile strength determination

As said, DPT was designed to indirectly measure the tensile strength of the concrete, therefore, using the definition of the test, some analytical expressions of the tensile strength are available in the literature. The maximum compression load and the dimensions of the test are the inputs in each analytical expression.

In [6], a limit analysis is applied idealizing concrete as a linear elastic-perfectly plastic material with very large ductility. The expression obtained is

$$f_t = \frac{P}{\pi(1.2\frac{d}{2}l - (\frac{d'}{2})^2)}.$$

Moreover, in order to be more accurate, they apply a finite element analysis considering concrete as an elastic plastic strain-hardening and fracture material. The final expression proposed is

$$f_t = \frac{0.75P}{\pi(1.2\frac{d}{2}l - (\frac{d'}{2})^2)}.$$

However, there are other analytical approximations of the tensile strength in the DPT given by different authors as follows.

Based on a nonlinear fracture mechanics approach, [8] proposed

$$f_t = 0.4\frac{P}{4(\frac{d}{2})^2}\sqrt{1+\frac{d}{\lambda d_a}}$$

where d_a is the maximum aggregate size and λ is an experimental parameter depending on the material. This expression is given in order to analyze the size effect of the specimen on the tensile strength value.

In [4] it is assumed a modified Coulomb-like failure criterion for concrete and

$$f_t = \frac{P}{\pi(\frac{d}{2}l - (\frac{d'}{2})^2\cot\alpha)}$$

considering $\alpha = \frac{\pi}{2} - \frac{\phi}{2}$ with ϕ being the shearing resistance angle in the modified Coulomb's yield criterion.

Finally, in [9] another analytical expression is presented

$$f_t = \frac{P}{9\pi l\frac{d'}{2}}.$$

However, we will only work with the expressions given in [6] and [9].

3 EXPERIMENTAL DATA

After an experimental campaign in the *Departament d'Enginyeria de la Construcció* of the *Universitat Politècnica de Catalunya (UPC)*, we have at our disposal experimental data. This experimental campaign consists of carrying out different tests considering the same concrete (i.e., the same material properties). Firstly, an uniaxial compression test is considered and, secondly, the Brazilian test is studied. However, the campaign was designed to study the double punch test. Hence, finally, the DPT is reproduced.

All the information is presented in table 1.

Herein, numerical models will be validated for the double punch test, considering the value of the maximum load obtained ($P = 1.52 \cdot 10^5$N) taking into account the rest of the information from the other tests.

Table 1: Experimental data

Description	Symbol	value	coment
Young's modulus	E	$35.5 \cdot 10^9 \mathrm{N/m^2}$	
Poisson ratio	ν	0.2	
Compressive strength	f_c	$50 \cdot 10^6 \mathrm{N/m^2}$ (2.69%)	from the uniaxial compression test
Tensile strength	f_t	$3.85 \cdot 10^6 \mathrm{N/m^2}$ (8.36%)	from the Brazilian test
Maximum load	P	$1.52 \cdot 10^5 \mathrm{N}$ (4.10%)	from the double punch test

4 PROBLEM STATEMENT

As seen, to characterize analytically the double punch test, we are only able to fit the relation between the tensile strength and the value of the maximum vertical load:

$$f_t \longleftrightarrow P.$$

Now, both numerical models must be validated, therefore, we need to compare the relation tensile strength - maximum vertical load obtained in the simulations with the analytic expressions. However, as seen in the previous section, there is scattering in the expressions relating the tensile strength with the maximum vertical load.

Hence, to validate both models, other tests with the same concrete (considering the same material parameters) are needed. These test must not present scattering in the determination of their interest quantities. As introduced in table 1, there are two tests carried out considering the same concrete in the experimental campaign: the uniaxial compression test and the Brazilian test.

4.1 Uniaxial compression test

The uniaxial compression test, presented in figure 3, consists in a concrete cylinder compressed both at the top and at the bottom. The load is applied in the whole surface of the top and the bottom of the specimen. The size of the specimen is fixed: $l = 30$ cm and $d = 15$ cm.

It is a direct compression test, therefore, it will provide us information of the concrete under compression: the compressive strength. Herein, the relationship between the compressive strength f_c and the maximum vertical load P is given by

$$f_c = \frac{4P}{\pi d^2}$$

where d stands for the diameter of the specimen.

Experimentally, the values obtained for this test are:

$$f_c = 50.45 \cdot 10^6 \mathrm{N/m^2} \longleftrightarrow P = 8.9 \cdot 10^5 \mathrm{N}.$$

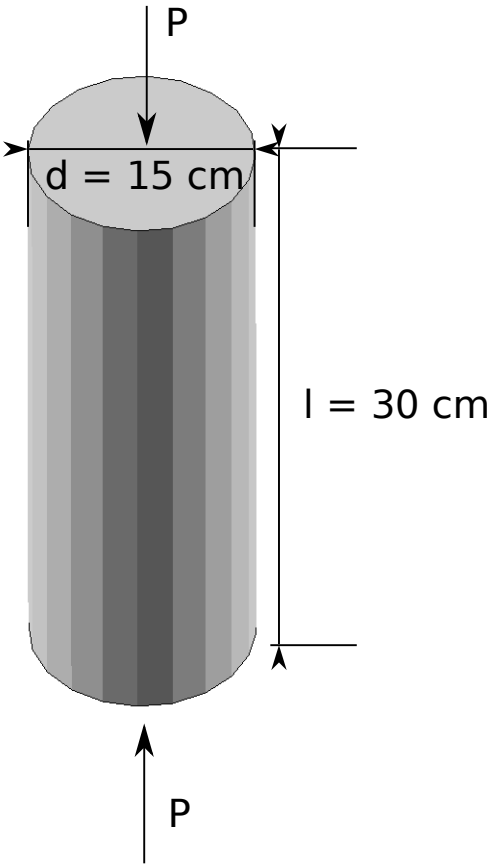

Figure 3: Description of the uniaxial compression test

4.2 Brazilian Test

The Brazilian test is an indirect tension test consisting in compressing a plain concrete cylinder placed horizontally by two steel punches (shown in figure 4).

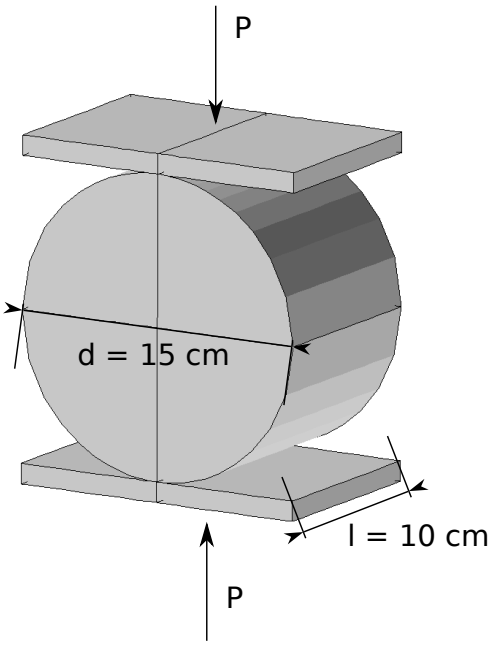

Figure 4: Description of the Brazilian test

For the Brazilian test, the relation between the tensile strength with the maximum vertical load is

given by

$$f_t = \frac{2P}{\pi l d}$$

where l and d stand for the length and the diameter of the concrete specimen, respectively.

The given analytic expression is standard and there is agreement about its accuracy. Hence, we validate the models for the double punch test through the Brazilian test.

From now on, the value of the tensile strength is fixed, then, in the Brazilian test, the maximum vertical load is also set.

$$f_t = 3.85 \cdot 10^6 \mathrm{N/m^2} \longleftrightarrow P = 8.6 \cdot 10^5 \mathrm{N}.$$

5 NUMERICAL MODELING

Two different techniques are considered, as said, to model plain concrete in the numerical simulation of the double punch test. Hence, both models may be validated for the double punch test considering the two tests described above.

5.1 Nonlocal Mazars damage model

In a damage model, the constitutive equation is given by $\boldsymbol{\sigma} = (1-D)\mathbb{C}\boldsymbol{\varepsilon}$, where D is a scalar parameter representing the damage and obeying $0 \leq D \leq 1$. If $D = 0$, the material is considered healthy and if $D = 1$, the material is completely damaged. In the above, $\boldsymbol{\sigma}$ and $\boldsymbol{\varepsilon}$ stand for stress and strain tensor, respectively. Moreover, $\mathbb{C}$ represents the elastic forth tensor.

The damage parameter evolves depending on y, $D = D(y)$, which is called *state variable* and depends on the strain field, $y = y(\varepsilon)$. Commonly, the damage starts when the state variable reaches a given threshold Y_0 and it always increases.

The Mazars Damage Model considers the damage parameter as a linear combination of the damage generated under tension, D_t, and the damage under compression, D_c,: $D = \alpha_t D_t + \alpha_c D_c$, considering

$$D_t = 1 - \frac{Y_0(1-A_t)}{\varepsilon} - A_t e^{-B_t(\varepsilon - Y_0)} \qquad \alpha_t = \sum_i \frac{\varepsilon_{ti}\langle\varepsilon_i\rangle}{\widehat{\varepsilon}^2}$$

$$D_c = 1 - \frac{Y_0(1-A_c)}{\varepsilon} - A_c e^{-B_c(\varepsilon - Y_0)} \qquad \alpha_c = \sum_i \frac{\varepsilon_{ci}\langle\varepsilon_i\rangle}{\widehat{\varepsilon}^2}$$

with $\alpha_t + \alpha_c = 1$ and

$$\langle\varepsilon_i\rangle = \frac{\varepsilon_i + |\varepsilon_i|}{2} \qquad \widehat{\varepsilon} = \sqrt{\sum_i \left(\frac{\varepsilon_i + |\,\varepsilon_i\,|}{2}\right)^2}$$

where ε_i are the main strains.

Moreover, ε_{ti} and ε_{ci} are calculated following the next scheme:

$$\boldsymbol{\sigma} \rightarrow \boldsymbol{\sigma}_{prin} \begin{cases} \boldsymbol{\sigma}^{+}_{prin} \rightarrow \boldsymbol{\sigma}^{+} \rightarrow \boldsymbol{\varepsilon}^{+} \rightarrow \boldsymbol{\varepsilon}^{+}_{prin} \rightarrow \boldsymbol{\varepsilon}_{ti} \\ \\ \boldsymbol{\sigma}^{-}_{prin} \rightarrow \boldsymbol{\sigma}^{-} \rightarrow \boldsymbol{\varepsilon}^{-} \rightarrow \boldsymbol{\varepsilon}^{-}_{prin} \rightarrow \boldsymbol{\varepsilon}_{ci} \end{cases}$$

with $\boldsymbol{\sigma} = \boldsymbol{\sigma}^{+} + \boldsymbol{\sigma}^{-}$ and $\boldsymbol{\varepsilon}_i = \boldsymbol{\varepsilon}_{ti} + \boldsymbol{\varepsilon}_{ci}$.

Herein, the damage follows an exponential law and the state variable is defined as $y = \varepsilon$, i.e., the damage is calculated in each point depending on the state variable $y = \varepsilon$ at the same point. However, this localization brings to a pathological mesh dependence and the results are not realistic. In order to solve this problem, a nonlocal damage model is considered, as introduced in [10]. The main idea of a nonlocal damage model is that the damage evolution depends on the state variable averaged in a neighborhood (associated to a characteristic length) of the current point, instead of depending on the state variable in the same point (as in a local model). Therefore a nonlocal state variable $\widetilde{y}$ is considered and it is defined as an average of the state variable in a neighborhood of each point. The characteristic lenght (l_{car}) is another material parameter and its function is to localize the nonlocality. In general, the value of the characteristic length is such that the neighborhood of each point involves two or three elements. Therefore, the nonlocal damage is $D = D(\widetilde{y})$. This is an integral nonlocal damage model because of the procedure employed for averaging the state variable, as seen in [11, 12].

Therefore, for the nonlocal Mazars damage model, six material parameters must be set:

- Damage threshold: Y_0
- Characteristic length: l_{car}
- Tension parameters: A_t and B_t
- Compression parameters: A_c and B_c

5.1.1 Uniaxial compression test

From the experimental campaign, we know the value of the compressive strength obtained through the uniaxial compression test, $f_c = 50.5 \cdot 10^6 \mathrm{N/m^2}$.

Considering the nonlocal Mazars damage model for the uniaxial compression test, we can consider that $D = D_c$, because the specimen is only under compression. Therefore, we can write the constitutive equation as

$$\sigma = \begin{cases} E \cdot \varepsilon & \varepsilon < Y_0 \\ (1 - D_c) \cdot E \cdot \varepsilon & \varepsilon \geq Y_0 \end{cases} = \begin{cases} E \cdot \varepsilon & \varepsilon < Y_0 \\ (\frac{Y_0(1-A_c)}{\varepsilon} + A_c e^{-B_c(\varepsilon - Y_0)}) \cdot E \cdot \varepsilon & \varepsilon \geq Y_0 \end{cases}.$$

Moreover, assuming that

$$\frac{\sigma}{\varepsilon}(\varepsilon_{max}) = 0 \quad \Longleftrightarrow \quad \sigma(\varepsilon_{max}) = f_c$$

a relationship between the compression parameters of the damage model (A_c and B_c) is found

$$A_c = \frac{B_c \cdot (Y_0 \cdot E - f_c)}{E \cdot (B_c \cdot Y_0 - e^{-1 + B_c \cdot Y_0})}$$

meanwhile, $B_c < \frac{1}{Y_0}$.

In figure 5, we can observe the damage model behavior under compression.

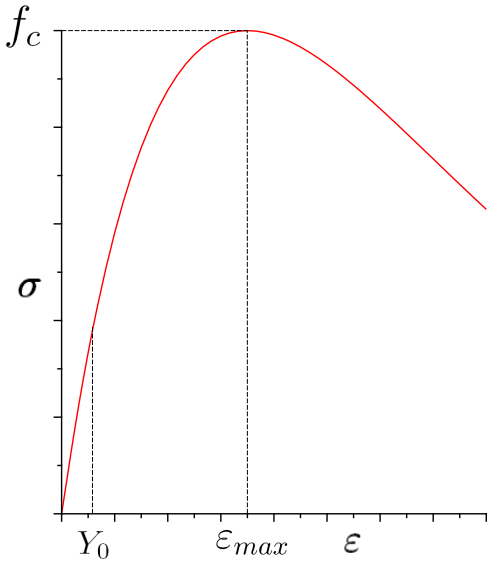

Figure 5: Description of the damage model under compression.

Therefore, through the uniaxial compression test, we are not able to evaluate any parameter, but we are able to set the relationship between the two compression parameters. Hence, when A_c and B_c satisfy the given equation, the value of the compressive strength is set (f_c).

5.1.2 Brazilian test

The value given by the experimental campaign from the Brazilian test is the tensile strength, $f_t = 3.84 \cdot 10^6 \mathrm{N/m^2}$.

In figure 6, the damage model is represented under tension.

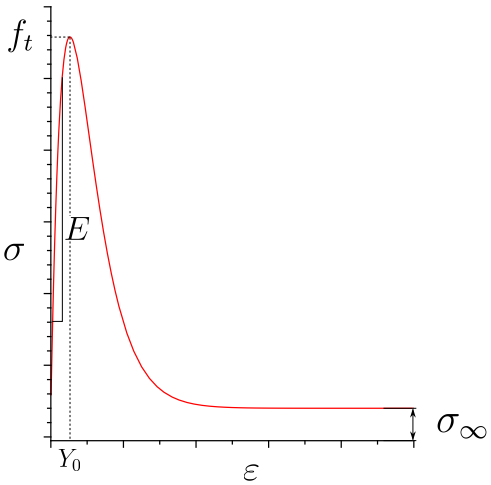

Figure 6: Description of the damage model under tension.

For this test, some consideration must be taken into account:

- $Y_0 = \dfrac{f_t}{E} = \dfrac{3.84 \cdot 10^6}{35.5 \cdot 10^9} = 1.08 \cdot 10^{-4}$
- the relationship obtained from the uniaxial compression test between A_c and B_c must be satisfied
- $A_c = 1 - \dfrac{\sigma_{\infty,c}}{E} < 1$, because the residual strength under compression is $\sigma_{\infty,c} \neq 0$
- $A_t = 1 - \dfrac{\sigma_{\infty,t}}{E} = 1$, because the residual strength under traction is $\sigma_{\infty,t} = 0$
- $B_t = 10000 \cdot (1 + \zeta)$, with $0 < \zeta < 1$, depending on the material
- $l_{car} = 2 \cdot 10^{-2}$m

Considering all this information and simulating numerically the test, all the material parameters are set and the value of the tensile strength obtained is the expected one (calculated through the value of the maximum vertical load). All the material parameters are presented in table 2.

Table 2: Optimal values of the material parameters of the nonlocal Mazars damage model for the Brazilian test

Material parameter	Value
Y_0	$1.08 \cdot 10^{-4}$
l_{car}	$2 \cdot 10^{-2}$m
A_t	1
B_t	10000
A_c	0.95
B_c	250

In order to analyze the fracture pattern of the Brazilian test, the damage distribution obtained carrying out the numerical simulation of the test is presented in figure 7.

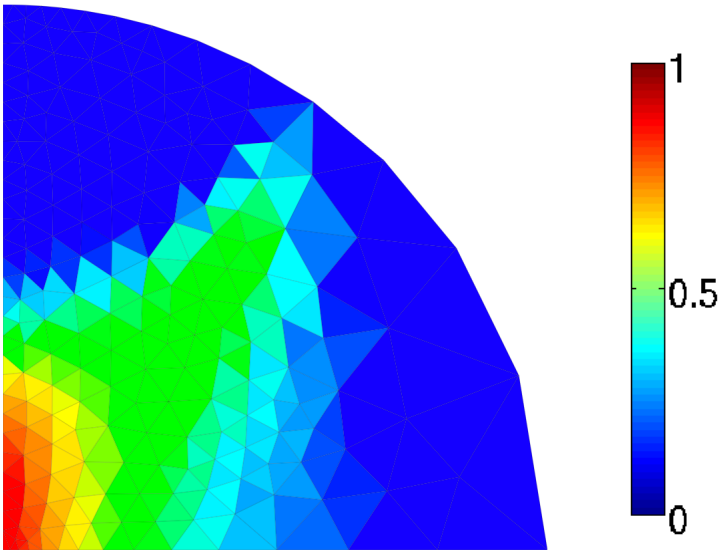

Figure 7: Damage distribution

5.1.3 Double punch test

Now, the double punch test is simulated considering the optimal material parameters combination from the Brazilian test. Herein, the value of the maximum vertical load obtained is $3.5 \cdot 10^5$N.

Moreover, in order to analyze the fracture pattern, the damage distribution obtained is presented in figure 8. It is observed both, the cone formation beneath the punch and four radial planes.

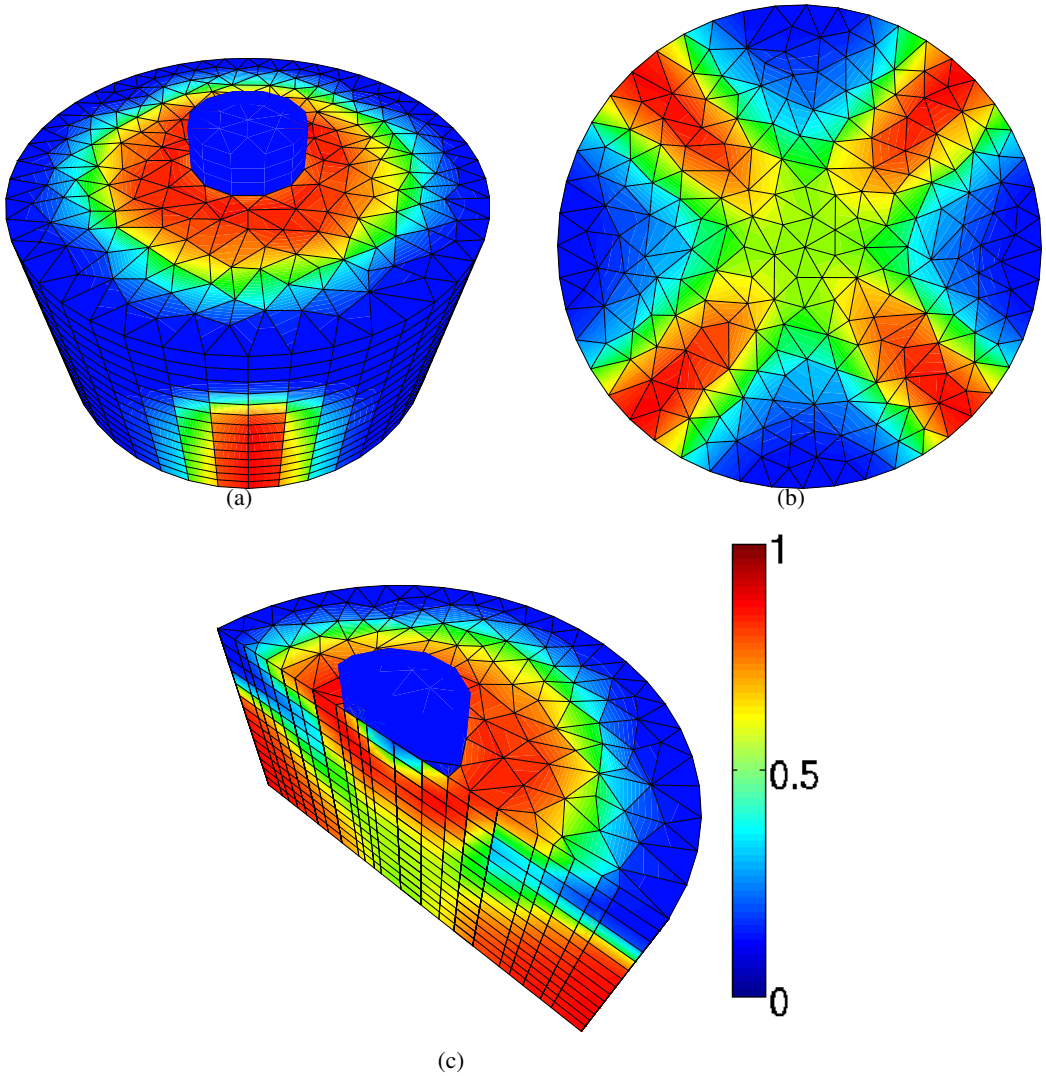

Figure 8: Damage distribution at the end of the simulation. (a) Top view. (b) Bottom view. (c) Inside view.

Although different meshes (for the same geometry) have been used with the numerical simulation of the double punch test considering the nonlocal Mazars damage model, the fracture pattern is always the same and placed as observed in figure 8.

5.2 Heuristic crack model with joints

An alternative to the damage model is a discontinuous model which considers the whole specimen as an elastic material and the cracking pattern defined using joint elements. In [13], all possible fracture paths are modeled using joint elements allowing any possible failure direction. Otherwise, in the double punch test, the cracking pattern is known a priori, therefore, only this cracking path is allowed (modeled using joint elements).

As introduced in [14, 15, 16], the nodes in the interface zone must be defined twice in order to define the joint elements, which will correspond to the duplicated geometry. Joint elements allow interfaces sliding and separation. The constitutive equations must incorporate both contact and noncontact conditions. When the interfaces are in contact, frictional sliding is possible, with dilatant behavior. The joint

model is ready to be incorporated in a standard nonlinear finite element code. It is easy because joint elements use the same type of nodal quantities as the continuous element.

Any constitutive equation modeling a joint element in a three-dimensional problem has three components. The first one corresponds to joint plane normal direction and the other two are the tangential directions of the plane. The normal one corresponds to the contact or separation between the joint interfaces. Meanwhile, the ones in the joint plane correspond to the slide directions.

The nonlinear behavior of joints is characterized by slide and separation taking place at the joint plane. For a joint with no tensile strength, separation of joint planes will occur when the tension normal to the joint plane becomes positive. Alternatively, a tensile strength can be given to the joint. If the shear strength of the joint is exceeded, irreversible slide occurs.

The Mohr-Coulomb Joint model is used to model the collapse pattern of a test. Therefore, the governing equations of the joint model for the numerical simulations can be written as

$$\sigma = k_{n1} \cdot u \quad \text{if} \quad \frac{-f_c}{k_{n1}} \leq u \leq \varepsilon_0 \tag{1}$$

$$\sigma = (k_{n1} \cdot \varepsilon_0 - k_{n2} \cdot \varepsilon_0) + k_{n2} \cdot u \quad \text{if} \quad u \geq \varepsilon_0 \tag{2}$$

$$\tau = -\tau_{max} \quad \text{if} \quad \frac{-\tau_{max}}{k_s} \leq v \tag{3}$$

$$\tau = k_s \cdot v \quad \text{if} \quad \mid v \mid \leq \mid \frac{\tau_{max}}{k_s} \mid \tag{4}$$

$$\tau = \tau_{max} \quad \text{if} \quad v \geq \frac{\tau_{max}}{k_s} \tag{5}$$

where $\tau_{max} = c + \sigma \tan(\varphi)$.

Table 3: Parameters of the model

Description	Symbol
first normal stiffness	k_{n1}
second normal stiffness	k_{n2}
strain threshold from k_{n1} to k_{n2}	ε_0
shear stiffness	k_s
maximum compressive strength	f_c
cohesion	c
friction angle	φ

In equations 1-5, applied stresses are divided into two components (normal (τ) and shear (σ)), and the displacements are also divided into u and v, corresponding to σ and τ, respectively. Moreover, in table 3, the relation between each parameter of the model and its meaning is presented.

In figure 9, it is shown (a) the relationship between stresses and displacements and (b) joint elements defined twice. There will be a normal component and two shear components with the same behavior, but in an orthogonal direction. Moreover, figure 10 reflects this constitutive law using two graphics: the normal (figure 10(a)) and shear (figure 10(b)) stresses.

Herein, due to its fracture pattern, the uniaxial compression test cannot be modeled using the heuristic cracking model. However, the information given by this test ($f_c = 50.45 \cdot 10^6 \mathrm{N/m^2}$) is used in order to fix the material parameters of this model.

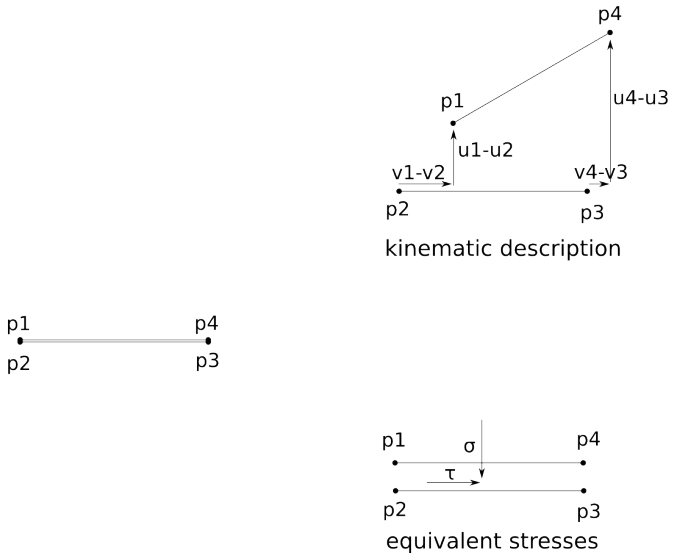

Figure 9: Stresses applied to a joint model and the corresponding displacements

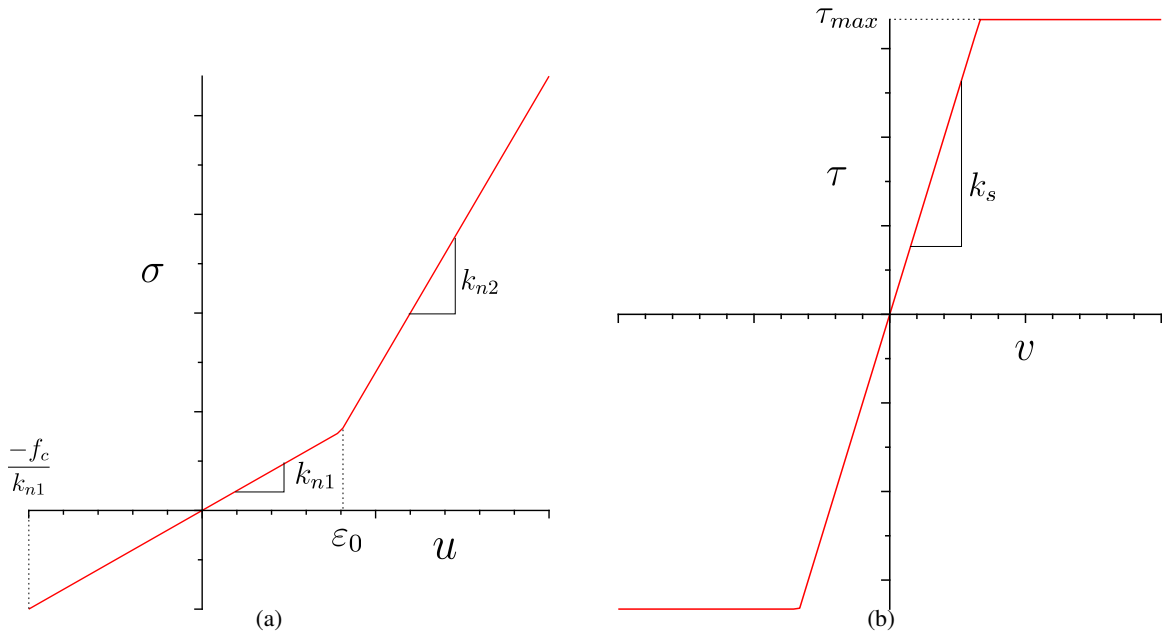

Figure 10: (a) σ and (b) τ evolution depending on the displacements

5.2.1 Brazilian test

Observing the damage distribution (figure 7), the Brazilian test is simulated modeling the cracking pattern with joint elements, meanwhile the rest of the specimen is considered elastic. In figure 11, joint elements are in red and the linear elements are black.

In table 4, all the material parameters of the joint elements for the Brazilian test, based on the experimental data ($f_t = 3.85 \cdot 10^6 \text{N/m}^2$ and $f_c = 50.45 \cdot 10^6 \text{N/m}^2$), are presented. Theses parameters must be different depending on the geometry, i.e., they are different whether they are vertical or inclined.

However, herein, a geometry parameter is not fixed: the height of the triangle. Hence, after carrying out some simulation of the Brazilian test considering all the material parameters fixed and different values of the triangle's height, we are able to capture the value of the maximum vertical load expected:

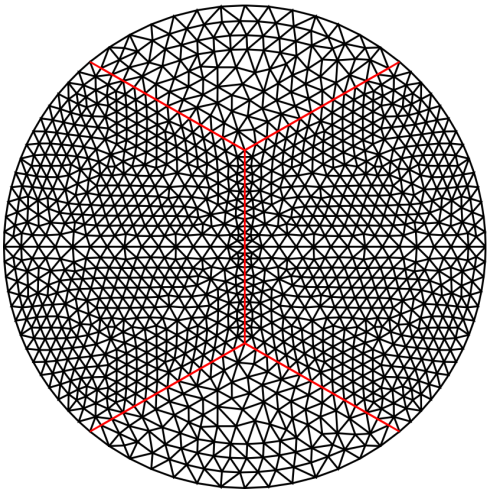

Figure 11: Brazilian test mesh for the discontinuous model

Table 4: Values of parameters for the Brazilian test

Symbol	for the vertical elements	for the inclined elements (in the triangle)
k_{n1}	$50 \cdot 10^7 \mathrm{N/m^3}$	$50 \cdot 10^{10} \mathrm{N/m^3}$
k_{n2}	$0 \mathrm{N/m^3}$	$50 \cdot 10^{13} \mathrm{N/m^3}$
ε_0	$\frac{3.85 \cdot 10^6}{50 \cdot 10^7}$	$\frac{3.85}{35.5} \cdot 10^{-3}$
k_s	$50 \cdot 10^{10} \mathrm{N/m^3}$	$50 \cdot 10^{10} \mathrm{N/m^3}$
f_c	$50 \cdot 10^6 \mathrm{N/m^2}$	$50 \cdot 10^6 \mathrm{N/m^2}$
c	$3.85 \cdot 10^6 \mathrm{N/m^2}$	$3.85 \cdot 10^6 \mathrm{N/m^2}$
φ	54^o	54^o

$P = 8.6 \cdot 10^5 \mathrm{N}$.

5.2.2 Double punch test

In order to simulate the double punch test considering the heuristic crack model with joints defined here, we consider two different meshes (as presented in figure 12): one with three radial planes and another with four radial planes.

Although double punch test is modeled in 3D, all joint elements are two-dimensional and triangular for the three planes and quadrilateral for the cone. The vertex of the cone is not included in the mesh because it would be a point defined too many times. Besides, three auxiliary planes are defined corresponding to the specimen's cracking planes, but inside the cone. They are necessary to define properly the joint elements. For the case of four radial planes, four auxiliary planes are defined inside the cone (corresponding to the intersection between the cone and the two diametral planes).

Again, all the material parameters are fixed (table 5) using the experimental data and taking into account whether they are inclined or not.

As in the previous test (Brazilian test), a geometry parameter is not fixed: the cone's height. Hence, in order to get the optimum cone's height value, different values for both three and four radial planes and the results are presented in figure 13. The optimum combinations are presented in table 6 considering the value of the maximum vertical load obtained in the simulation. The optimum value of the cone's hight is the one which corresponds to the highest value of the maximum vertical load, i.e., the nearest to the

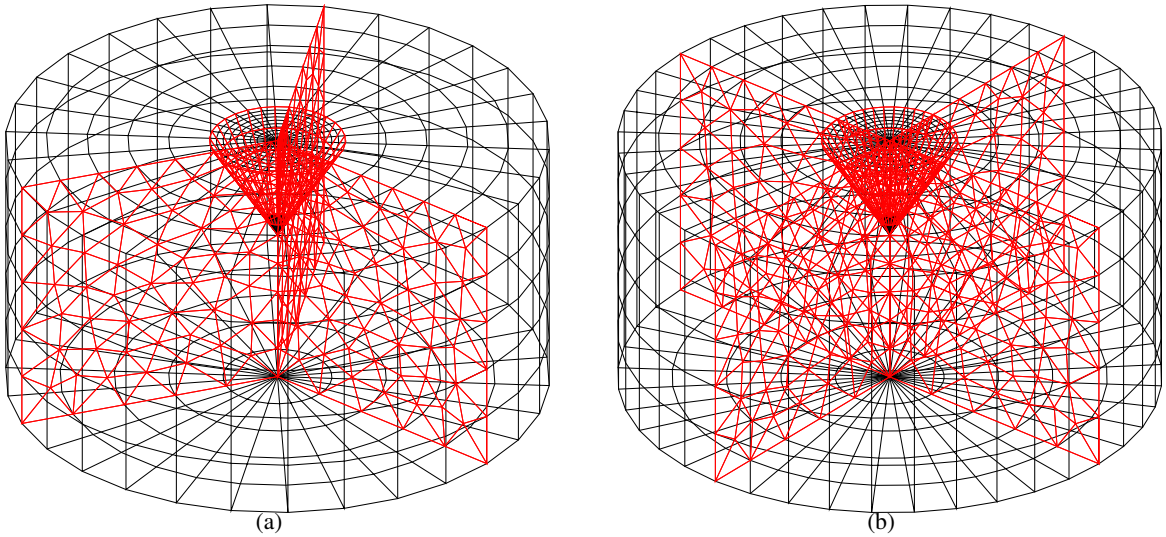

Figure 12: Double punch test including joint elements meshes. (a) three radial cracking planes. (b) four radial cracking planes.

Table 5: Values of parameters for the double punch test

Symbol	for the meridian planes	for the cone	for the auxiliary planes in the cone
k_{n1}	$50 \cdot 10^7 \mathrm{N/m^3}$	$50 \cdot 10^{10} \mathrm{N/m^3}$	$30 \cdot 10^{15} \mathrm{N/m^3}$
k_{n2}	$0 \mathrm{N/m^3}$	$50 \cdot 10^{13} \mathrm{N/m^3}$	$30 \cdot 10^{15} \mathrm{N/m^3}$
ε_0	$\frac{3.85 \cdot 10^6}{50 \cdot 10^7}$	$\frac{3.85}{35.5} \cdot 10^{-3}$	$\frac{3.85}{35.5} \cdot 10^{-3}$
k_s	$50 \cdot 10^{10} \mathrm{N/m^3}$	$50 \cdot 10^{10} \mathrm{N/m^3}$	$30 \cdot 10^{15} \mathrm{N/m^3}$
f_c	$50 \cdot 10^6 \mathrm{N/m^2}$	$50 \cdot 10^6 \mathrm{N/m^2}$	$50 \cdot 10^6 \mathrm{N/m^2}$
c	$3.85 \cdot 10^6 \mathrm{N/m^2}$	$3.85 \cdot 10^6 \mathrm{N/m^2}$	$3.85 \cdot 10^6 \mathrm{N/m^2}$
φ	54^o	54^o	54^o

analytical values.

Table 6: Optimal cracking patterns

Number of cracking planes	cone's height	Maximum vertical load
3	$3.5 \cdot 10^{-2} \mathrm{m}$	$1.50 \cdot 10^5 \mathrm{N}$
4	$3 \cdot 10^{-2} \mathrm{m}$	$1.25 \cdot 10^5 \mathrm{N}$

6 VALIDATION

Considering $f_c = 50.45 \cdot 10^6 \mathrm{N/m^2}$ and $f_t = 3.85 \cdot 10^6 \mathrm{N/m^2}$ fixed, in table 7 all the results are presented and compared. Firstly, the analytical expressions are presented with their corresponding maximum vertical load. Moreover, the numerical results are presented obtained with all the different methods. Finally, numerical results are compared with each analytical value (last 3 columns). The errors in the comparison are calculated considering all the three analytical values.

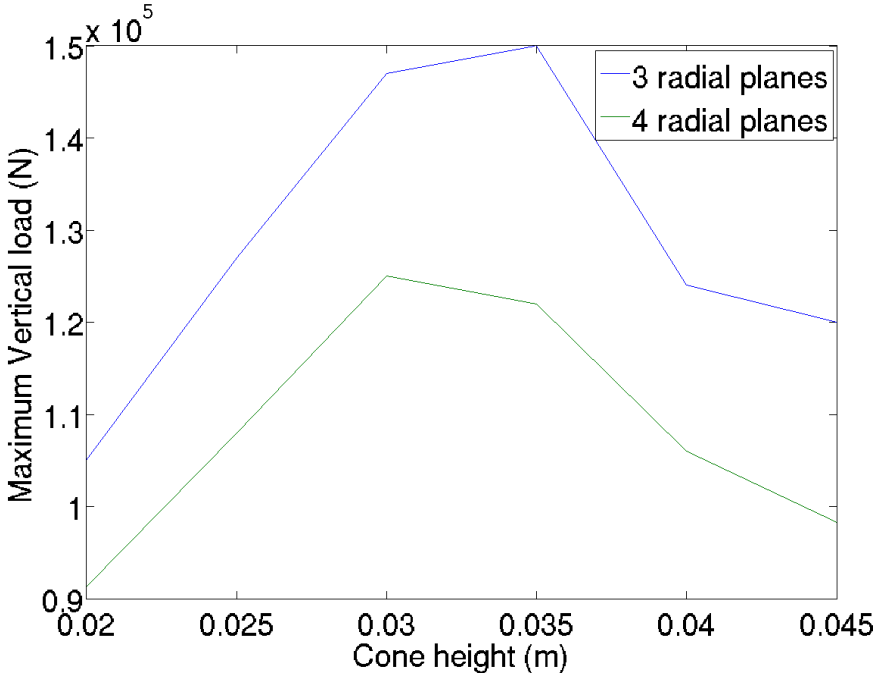

Figure 13: Maximum vertical load evolution considering different values of the cone's height.

Table 7: Model Validation

Description	P (N)	$\varepsilon_1 = \left\lvert \frac{P_{ref1} - P_i}{P_{ref1}} \right\rvert$	$\varepsilon_2 = \left\lvert \frac{P_{ref2} - P_i}{P_{ref2}} \right\rvert$	$\varepsilon_3 = \left\lvert \frac{P_{ref3} - P_i}{P_{ref3}} \right\rvert$
$f_t = \frac{P}{\pi(1.2bH - a^2)}$	$1.51 \cdot 10^5$	P_{ref1}		
$f_t = \frac{0.75P}{\pi(1.2bH - a^2)}$	$2.01 \cdot 10^5$		P_{ref2}	
$f_t = \frac{P}{\pi 9Ha}$	$1.45 \cdot 10^5$			P_{ref3}
Continuous model	$3.5 \cdot 10^5$	1.3	0.74	1.4
Discontinuous model 3 planes ($h = 3.5 \cdot 10^{-2}$m)	$1.50 \cdot 10^5$	0.006	0.25	0.03
Discontinuous model 4 planes ($h = 3 \cdot 10^{-2}$m)	$1.25 \cdot 10^5$	0.17	0.38	0.14

7 CONCLUDING REMARKS

- After modeling the double punch test considering two different numerical models, both models are validated through the uniaxial compression test and the Brazilian test.
- All the parameters (both the material and the geometrical ones) are set for both numerical models.
- A material parameter combination is considered for the nonlocal Mazars damage model. However, it is not proved that it is unique.
- Not all the material parameters of the nonlocal Mazars damage model have a physical meaning.
- After trying different material combinations for the nonlocal Mazars damage model, always taking into account all of the conditions found during the present work, we can say that there is only one degree of freedom in order to get the value of the maximum vertical load which is A_c (or B_c). Different values of the other parameters, have no sense or they do no effect in the value of the

maximum vertical load. Hence, we may be able to find a different value of A_c, which gives a different value of the maximum vertical load closer to the experimental one. In this case, we would have the same model, but with different material parameters for two different test with the same concrete, which may be due to their fracture pattern.

- The most suitable model is the discontinuous one because the error is smaller considering the 3 cracking radial planes. Moreover, the error is smaller comparing the values with all the analytical ones.

- However, using the joint model, it is necessary to know the fracture patter before the simulation. Meanwhile, with the nonlocal Mazars damage model, the failure pattern is not set a priori.

- Time calculation and computational cost are shorter using the discontinuous model than with the nonlocal Mazars damage model, due to the number of nonlinear elements in each model.

- Both the nonlocal Mazars damage model and the model including joint elements in the fracture pattern have been validated for the DPT, which was designed for studying the tensile strength (f_t) of concrete. Therefore, these numerical simulations allow to control f_t, for any material parameters considering both models.

  - For the nonlocal Mazars damage model, given the damage threshold (Y_0) and the Young modulus (E), it is possible to get f_t, using the relation $Y_0 = \dfrac{f_t}{E}$.
  - Otherwise, for the model using joint elements, concrete's tensile strength (f_t), can be set with the strain threshold from k_{n1} to k_{n2}, defined as $\varepsilon_0 = \dfrac{f_t}{E}$. Therefore, using the threshold and the Young's modulus, the tensile strength is controlled.

- Up to now, the double punch test has been simulated numerically for plain concrete. Then our next step will be including fibers into these models in order to simulate the double punch test for steel fiber reinforced concrete (a test introduced in [17] and [18], defined as the Barcelona Test).

REFERENCES

[1] K. T. Chau, X. X. Wei. "Finite solid circular cylinders subjected to arbitrary surface load. Part I: Analytic solution". *International Journal of Solids and Structures.*, Vol. **37**, 5707-5732, 2000.

[2] K. T. Chau, X. X. Wei. "Finite solid circular cylinders subjected to arbitrary surface load. Part II: Application to double-punch test". *International Journal of Solids and Structures.*, Vol. **37**, 5733-5744, 2000.

[3] A. Rodríguez-Ferran, A. Huerta. "Error estimation and adaptivity for nonlocal damage models", *International Journal of Solids and Structures.*, Vol. **37**, 7501-7528, 2000.

[4] L. Bortolotti. "Double-punch test for tensile and compressive strengths in concrete". *IACI Materials Journal.*, Vol. **85-M4**, 26-32, 1988.

[5] W. F. Chen. "Double punch test for tensile strength of concrete". *ACI Mater J.*, Vol. **67 (2)**, 993-995, 1970.

[6] W. F. Chen, R. L. Yuan. "Tensile strength of concrete: Double punch test". *Journal of structural divisions, ASCE.*, Vol. **106**, 1673-1693, 1980.

[7] W. F. Chen, B. E. Ttumbauer. "Double-punch test and tensile strength of concrete". *Journal of Materials, American Society of testing and materials.*, Vol. **7 (2)**, 148-154, 1972.

[8] P. Marti. "Size effect in double-punch test on concrete cylinders". *ACI Materials Journal.*, Vol. **86-M58**, 597-601, 1989.

[9] S. Saludes, A. Aguado, C. Molins. "Ensayo de doble punzonamineto aplicado al homrigón reforzado con fibras (ensayo Barcelona)" *Publicacions del departament enginyeria de la contrucció, ETSECCPB, UPC*. 2006.

[10] M. Jirásek. "Nonlocal damage mechanics". *Damage and fracture in geomaterials.*, Vol. **11**, 993-1021, 2007.

[11] G. Pijaudier-Cabot, A. Huerta. “Finite element analysis of bifurcation in nonlocal strain softening solids”. *Computer Methods in Applied Mechanics and Engineering.*, Vol. **90**, 905-919, 1991.

[12] A. Rodriguez-Ferran, A. Huerta. “Error estimation and adaptivity for nonlocal damage models”. *International Journal of Solids and Structures.*, Vol. **37**, 7501-7528, 2000.

[13] C. M. López, I. Carol, A. Aguado. “Estudio de la fractura del hormigón mediante un modelo numérico micromecánico con elementos junta”. *MECOM 99.*, Mendoza, Argentina. September 6-10, 1999.

[14] P. Díez, P. Pegon. “Error assessment of structural computations including joints”. *Fifth World Congress on Computational Mechanics.*, Vienna, Austria. July 7-12, 2002.

[15] G. Beer. “An isoparametric joint/interface element for finite element analysis”. *International Journal For Numerical Methods in Engineering.*, Vol. **21**, 585-600, 1985.

[16] M. F. Snyman, W. W. Bird, J. B. Martin. “A simple formulation of a dilatant joint element governed by Coulomb friction”. *Engineering Computations.*, Vol. **8**, 215-229, 1991.

[17] C. Molins, A. Aguado, S. Saludes, T. Garcia. “New test to control tension properties of FRC”. *ECCOMAS Thematic Conference on Computational Methods in Tunnelling (EURO:TUN 2007).*, Vienna, Austria, August 27-29, 2007.

[18] C. Molins, A. Aguado, S. Saludes. “Double Punch Test to control the energy dissipation in tension of FRC (Barcelona Test)”. *Materials and Structures.*, Vol. **42**, 415-425, 2009.